

# Coiled-Fiber Sensor for Vectorial Measurement of Magnetic Field

Valerio Annovazzi-Lodi, *Member, IEEE*, Silvano Donati, *Member, IEEE*, and Sabina Merlo

**Abstract**—We derive new results on the polarization properties of a matched fiber-coil (i.e., one beat length per turn) immersed in a magnetic field. We show that both components  $H_y$  and  $H_z$ , perpendicular to the coil axis, can be simultaneously measured. Sensing coils of 1-cm diameter, with multiple turns of fiber have been fabricated. Using 100-turn heads, we have achieved a sensitivity of 0.01 Gauss for the vectorial fiber sensor.

## I. INTRODUCTION

RECENTLY, applications to the electrical industry of fiber-optic sensors based on the Faraday effect have attracted a considerable interest [1]–[4], and field trials of various electrical current sensors have been reported. However, less attention has been paid so far to magnetic field fiber sensors for the diagnostics of high-power electrical machinery, such as transformers and generators in power plants. For instance, an important issue is the early detection of short circuit in a single turn (or in a few turns) of the machine winding. For this purpose, an array of point-like magnetic field sensors has to be installed around the winding to monitor the distribution of stray flux and its short-circuit-induced distortions.

With respect to their conventional (electrical) counterparts, fiber-optic sensors have the well-known advantages of a completely passive and insulating structure, and of a high degree of EMI immunity; however, they fall short on other specifications for the magnetic sensing application, such as the required sensitivity (down to 0.01 Gauss) and dynamic range (hundreds of Gauss), as well as the small size (about 1 cm).

We have developed an all-fiber magnetic field sensor which meets all these requirements. The sensing element is a coil of low-birefringence fiber, wound with a carefully adjusted curvature radius  $R$ , so that the beat length  $L_b = 2\pi/\beta$  of the bending-induced birefringence matches the loop perimeter  $2\pi R$ . In this way, as known from previous papers [1], [5]–[7], the Faraday rotation is cumulated even on opposite half-turns, instead of being canceled as in an ideal (i.e., zero linear birefringence) fiber coil placed in a uniform magnetic field.

However, one should carefully avoid even small radius errors, which become intolerable when cumulated on hundreds of turns. Therefore, we have first analyzed the problem of constant linear birefringence superposed to periodic Faraday

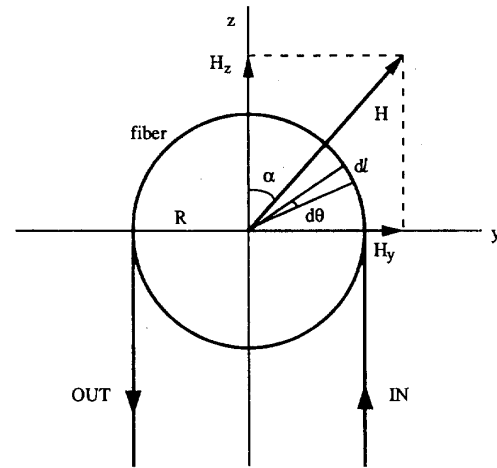


Fig. 1. Geometry of a coiled fiber in a uniform magnetic field.

rotation in presence of a radius mismatch ( $R \neq 1/\beta$ ), and we have found results well fitted by experimental data. Then, we show that the  $VL$  product (Verdet constant  $V$  by fiber length  $L$ ) can be increased hundredfold in a matched coil, thus surpassing the  $VL$  product of YIG crystal used in microoptic magnetic field sensors [1], [8].

## II. THEORY

We consider a fiber coil immersed in a uniform magnetic field  $H$ , as in Fig. 1. The Jones matrix  $\underline{J}$  for the elemental length  $dl = R d\theta$  along the fiber (being  $\theta$  the angle along the loop of radius  $R$ ) is defined by

$$\underline{E}(l + dl) = \underline{J} \cdot \underline{E}(l) \quad (1)$$

and can be expressed [6], [9], as

$$\underline{J} = \underline{I} + \underline{M} dl \quad (2)$$

where

$$\underline{M} = \begin{bmatrix} i\beta & VH \cos(l/R + \alpha) \\ -VH \cos(l/R + \alpha) & 0 \end{bmatrix}, \quad (3)$$

$\underline{I}$  is the identity matrix,  $\beta$  is the distributed linear birefringence in the fiber due to bending,  $H$  is the magnetic field,  $V$  is the Verdet constant of the fiber, and  $\alpha$  is the angle between the vector  $H$  and the input wavevector.

Substituting (3) in (1) yields

$$d/dl \underline{E} = \underline{M} \cdot \underline{E}. \quad (4)$$

Manuscript received October 22, 1991. This work was supported by the Italian National Research Council (C.N.R.-Progetto Finalizzato Tecnologie Elettrotelegrafiche).

The authors are with the Dipartimento di Elettronica, Università di Pavia, Via Abbiategrasso 209, I-27100 Pavia, Italy.

IEEE Log Number 9202097.

This is a set of nonlinear differential equations, that should be solved with the input boundary condition, in order to obtain the Jones matrix  $\underline{J}_o$  relating the input and output Jones vectors  $\underline{E}_i \equiv [E_{xo}, E_{yo}]$  and  $\underline{E}_o \equiv [E_x, E_y]$  as

$$\underline{E}_o = \underline{J}_o \cdot \underline{E}_i. \quad (5)$$

We have found that (4) can be converted to a Riccati's equation [6] and therefore, in the general case, it cannot be solved in a closed form. However, under the assumption  $VH \ll 1/\beta$ , a solution is obtained in the special case of an integer or semiinteger number  $N$  of turns in the coil, if the loop perimeter  $2\pi R$  is an exact multiple of the beat length ( $\beta = n/R$ ).

Limiting ourselves to the most interesting case  $n = 1$ , and with the position

$$\Phi = VHR\pi N$$

the solution for small  $\Phi$  is

$$\underline{J}_o = \begin{bmatrix} 1 & \Phi \exp(i\alpha) \\ -\Phi \exp[-i(\alpha + 2N\pi)] & \exp[i(2N\pi)] \end{bmatrix}. \quad (6)$$

From (6), if the magnetic field is parallel to the direction of the input light propagation, i.e.,  $H = H_z$  ( $\alpha = 0$ ), we find

$$\begin{aligned} E_x &= (E_{xo} + VH_z\pi NRE_{yo}) \\ E_y &= (-1)^{2N}(E_{yo} - VH_z\pi NRE_{xo}) \end{aligned} \quad (7a)$$

thus, the birefringence effect consists in a pure rotation of an angle  $\Phi_z = VH_zR\pi N$ , which is exactly one half of the expected Faraday rotation for a straight fiber of length  $2\pi NR$ .

If, instead, the magnetic field is orthogonal to the direction of the input light propagation, that is  $H = H_y$  ( $\alpha = \pi/2$ ), then

$$\begin{aligned} E_x &= (E_{xo} + iVH_y\pi NRE_{yo}) \\ E_y &= (-1)^{2N}(E_{yo} + iVH_y\pi NRE_{xo}) \end{aligned} \quad (7b)$$

and the coil acts as a linearly birefringent plate with retardance  $\Phi_y = VH_yR\pi N$  and principal axes oriented at  $\pm 45^\circ$  with respect to the  $xy$  frame.

Since rotation and linear birefringence are orthogonal displacements on the Poincaré sphere, they are linearly superposed for small angles  $\Phi_y$ ,  $\Phi_z$ , and can be measured simultaneously. Fig. 2 shows a simple, double polarimetric scheme for the readout of  $H_y$  and  $H_z$  components. Here, the output radiation is divided by a beamsplitter (BS), and in-phase and in-quadrature components are measured in the two arms. The in-phase component is detected by a polarizer oriented at  $45^\circ$  with respect to the input polarization, while a quarter wave retarder is used before a polarizer to sense the in-quadrature component. The output photodetected currents  $I_y$  and  $I_z$  are

$$I_y = I_o \cos^2(45^\circ + \Phi_y) = (I_o/2)(1 - \sin 2\Phi_y) \quad (8a)$$

$$I_z = I_o \cos^2(45^\circ + \Phi_z) = (I_o/2)(1 - \sin 2\Phi_z) \quad (8b)$$

and, for small values of the magnetic field, the signals around the quiescent value ( $I_o/2$ ) are linearly related to  $\Phi_y$  and

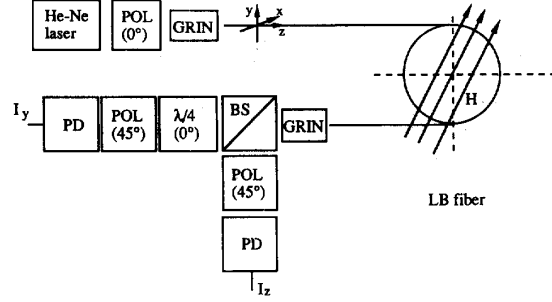


Fig. 2. Magnetic field sensor based on the one-wavelength-per-turn linear birefringence: polarimetric dual channel detection scheme for measuring both  $H_y$  and  $H_z$  magnetic field components. (PD = Photodiode, BS = beamsplitter, POL = polarizer, between parentheses the inclination angle).

$\Phi_z$ :  $\Delta I_y \approx -2\Phi_y$ ,  $\Delta I_z \approx -2\Phi_z$ . In addition, slightly modified readout schemes [1] can be used for dynamic range extension and linearity improvement.

Now, a critical issue to be analyzed is the sensitivity to the matching condition of one beat length per turn. To evaluate the imperfect matching, we take

$$\beta = (1/R) + \varepsilon \quad (9)$$

where  $\varepsilon$  is the mismatch error. With a perturbational method, we have solved (4) in the small signal condition  $HV \ll \beta$ . We assume that a small Faraday rotation is added to the linear birefringence of the coil, which is considered as the main effect. As a trial solution we write

$$\underline{E}_o = \begin{bmatrix} \exp(i\beta l) & 0 \\ 0 & 1 \end{bmatrix} \cdot \underline{E}_i + \underline{e}_o \quad (10)$$

where  $\underline{e}_o = [e_x, e_y]$  is the perturbation vector to be determined. By substituting (10) into (4), after some manipulations, we obtain a set of linear differential equations in the vector  $\underline{e}_o$ , which can be solved with the following result:

$$\begin{aligned} e_x &= -iE_{yo}(VH/2) \exp(i\beta l) \\ &\cdot \left\{ -\frac{R}{1 + \beta R} \left\{ \exp[-i(l/R + \beta l + \alpha)] - \exp(-i\alpha) \right\} \right. \\ &\quad \left. + \frac{R}{1 - \beta R} \left\{ \exp[i(l/R - \beta l + \alpha)] - \exp(i\alpha) \right\} \right\} \end{aligned} \quad (11a)$$

$$\begin{aligned} e_y &= -iE_{xo}(VH/2) \\ &\cdot \left\{ -\frac{R}{1 + \beta R} \left\{ \exp[i(l/R + \beta l + \alpha)] - \exp(i\alpha) \right\} \right. \\ &\quad \left. + \frac{R}{1 - \beta R} \left\{ \exp[-i(l/R - \beta l + \alpha)] - \exp(-i\alpha) \right\} \right\}. \end{aligned} \quad (11b)$$

Substituting (11) and (9) into (10), normalizing to unit the determinant of  $\underline{J}_o$  and neglecting an inessential phase factor yield

$$\underline{J}_o \approx \begin{bmatrix} \cos \phi \exp(i\Delta) & Q \sin \phi \\ -Q^* \sin \phi & \cos \phi \exp(-i\Delta) \end{bmatrix} \quad (12)$$

at the first order in  $\epsilon$ , where:

$\Delta = \beta l/2$  is the linear birefringence retardance for the considered length  $l$ ,

$\phi = VHl/2$  is the Faraday angle, i.e., the polarization rotation that would be measured in a straight fiber length  $l/2$ ,

$Q = \{[\exp i(\Delta - \mu + \alpha)] \text{sinc } \mu\} + \{[\exp -i(\Delta - \mu + \alpha)] \text{sinc}(2\Delta - \mu)\}$ , and  $\mu = \epsilon l/2$  is the phase error due to radius mismatch.

It is interesting to decompose  $\underline{J}_o$  in a pure rotation  $R$  preceded and followed by pure linear retardances  $B$  and  $B'$ . By letting

$$\underline{J}_o = \underline{B} \underline{R} \underline{B}' \quad (13)$$

and equating term by term, we obtain, for  $\Delta \gg 1$  and small  $\Phi$ , the matrices

$$\underline{B} = \begin{bmatrix} \exp\{i[\Delta - (\mu - \alpha)/2]\} & 0 \\ 0 & \exp\{-i[\Delta - (\mu - \alpha)/2]\} \end{bmatrix} \quad (14a)$$

$$\underline{R} = \begin{bmatrix} \cos(\phi \text{sinc } \mu) & \sin(\phi \text{sinc } \mu) \\ -\sin(\phi \text{sinc } \mu) & \cos(\phi \text{sinc } \mu) \end{bmatrix} \quad (14b)$$

$$\underline{B}' = \begin{bmatrix} \exp[i(\mu - \alpha)/2] & 0 \\ 0 & \exp[-i(\mu - \alpha)/2] \end{bmatrix}. \quad (14c)$$

Equations (14) show that, after  $N$  turns, a mismatch from the tuning condition  $\epsilon = 0$  results not only in a reduction of the Faraday angle by a factor  $\text{sinc } \mu$  (matrix  $\underline{R}$ ), but also in a variation of the double linear birefringence effect expressed by matrices  $\underline{B}$  and  $\underline{B}'$ . The contribution of  $\underline{B}'$  can be always avoided by entering along a principal axis, while the effect of the detuning on  $\underline{B}$  should be compensated at the output. This can be done at a convenient  $\alpha$ , for example  $\alpha = 0$ ; then the output fields are still given by (7) provided that the angle  $\Phi$  is reduced by a factor  $\text{sinc } \mu$ .

The expressions of the output currents  $I_y$  and  $I_z$  as a function of the trimming error  $\mu$  can be obtained from (12) or (14). A moderate mismatch from the tuning condition (small  $\epsilon$ ) results in two additional terms in (8) and we find for the signal components:

$$\Delta I_y = -(I_0/2) \text{sinc } \mu [\cos \mu \sin 2\Phi_y + \sin \mu \sin 2\Phi_z] \quad (15)$$

$$\Delta I_z = -(I_0/2) \text{sinc } \mu [\cos \mu \sin 2\Phi_z - \sin \mu \sin 2\Phi_y]. \quad (16)$$

These equations show for both parallel ( $\alpha = 0$ ) and orthogonal input ( $\alpha = \pi/2$ ) not only a reduction of responsivity by a factor  $(\cos \mu \text{sinc } \mu) = \text{sinc}(2\mu)$  but also a crosstalk from the other channel. The cross talk rejection ratio can be computed from (15), (16), and amounts to  $1/tg\mu$ .

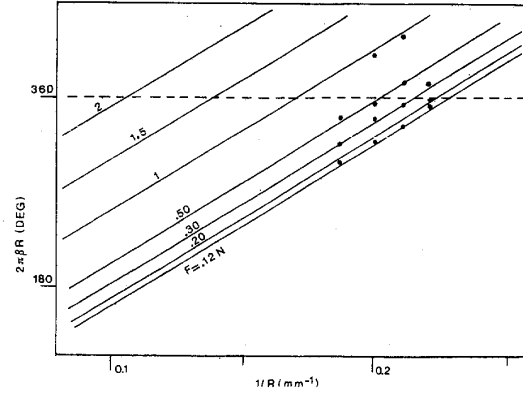


Fig. 3. One turn phase delay  $\Delta\Phi = 2\pi\beta R$  due to superposition of bending and tension in a low-birefringence optical fiber (York LB 800). Straight lines are computed from fiber parameters and dots are experimental values.

### III. SENSOR DESIGN

We have made several sensor heads consisting of  $N = 1.5 - 170$  loops of low-birefringence fiber York LB 800 (measured Verdet constant  $V = 4.5 \mu\text{rad}/\text{A} = 3.6 \cdot 10^{-4} \text{ rad}/\text{G} \cdot \text{m}$ , at 633 nm). A 633 nm He-Ne laser was used as a source, yet the fiber worked efficiently in single-mode regime due to the differential bending attenuation between the fundamental and the higher order modes. Different combinations of bending and tension birefringence can be selected to match the beat-length per-turn condition. Writing the linear birefringence as  $\beta = (K/R^2) + (K'F/R)$  [9], where  $F$  is the tension force, the retardance  $\Delta\Phi = 2\pi\beta R$  per turn becomes

$$\Delta\Phi = 2\pi[(K/R) + K'F]. \quad (17)$$

Fig. 3 shows experimental data fitting (17) for the fiber in use. In the sensor design, we preferred to limit mechanical tension for improving long term reliability, and to reduce the radius for better compactness, finally selecting  $R = 4.5 \text{ mm}$  with  $F = 0.3 \text{ N}$ . After trimming, the coil was cemented with epoxy glue. Several coils ( $\approx 50$ ) were fabricated, and neither failures nor degradation were observed over a 6-month period.

Different samples were made to test the repeatability of the winding process. The maximum useful fiber length was found to be limited mainly by the cumulative birefringence error, while the bending attenuation was relatively small. In practice, we achieved a number of loops of  $N = 170$  by carefully avoiding kinks and accurately controlling the bending tension. Such sensor heads were about 20 mm long and gave adequate responsivity for the measurement on standard electrical machinery.

The insulating properties of our probes were limited by surface discharge along the downlead fiber trunks; typical values of the withstanding voltage for our magnetic field meters were in the range 50–100 KV.

Fig. 4 shows the response of a sensor head ( $N = 44$ ), with the expected linear trend at relatively low magnetic field amplitudes. Saturation for  $H > 4 \text{ KG}$  comes from the  $\sin 2\Phi$  dependence in (8); this nonlinearity can be corrected by several well-known schemes [1].

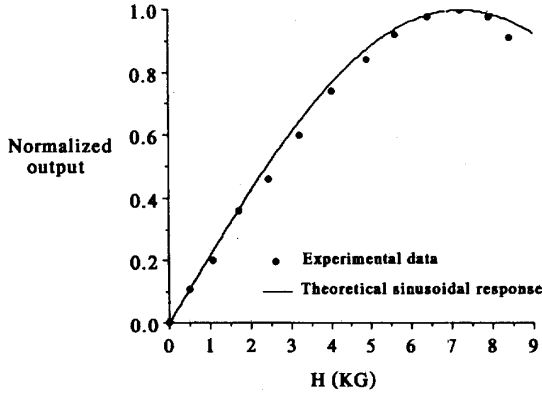


Fig. 4. Normalized response of a 44-loop magnetic field sensor as a function of the measured field.

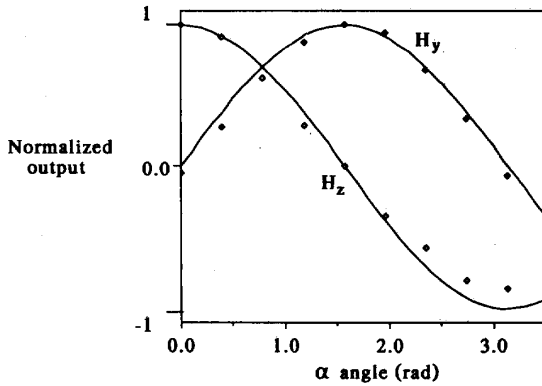


Fig. 5. Magnetic field components  $H_y$  and  $H_z$  as a function of the orientation angle  $\alpha$ , showing the vectorial response of the fiber sensor.

In Fig. 5 the two components  $H_y$ ,  $H_z$  are plotted versus the orientation angle  $\alpha$  for a value of  $H$  within the linearity range ( $H \approx 1$  KG). The experimental points are fitted by the theoretical  $\sin \alpha$  and  $\cos \alpha$  dependence, which demonstrates the simultaneous measurement of two independent magnetic field components.

The noise performance of the sensor can be expressed in terms of the noise equivalent magnetic field (NEH), defined as the magnetic field that would give an output signal equal to the noise level (i.e.,  $S/N = 1$ ). For a matched coil, we have found [1] that

$$NEH = (2eI_0B)^{1/2} / (I_0VRN\pi). \quad (18)$$

It follows that the theoretical sensitivity limit can be as low as  $1.3 \cdot 10^{-4} \text{ G}/(Hz)^{1/2}$  for our setup, with  $N = 100$  and  $I_0 = 100 \mu\text{A}$ . Using a standard transresistance amplifier scheme, shot noise limited regime was achieved in most of the frequency range of operation, from low frequency to over 1 MHz. In a typical laboratory environment, without special care in decoupling the sensor head, we reached a sensitivity of about  $10^{-2} \text{ G}$  at line frequency ( $B = 45$  to  $55 \text{ Hz}$ ,  $I_0 = 12 \mu\text{A}$ ) and of about 3 G for the full available bandwidth ( $B = 1 \text{ MHz}$ ), which was limited by the electronics. It should be pointed out,

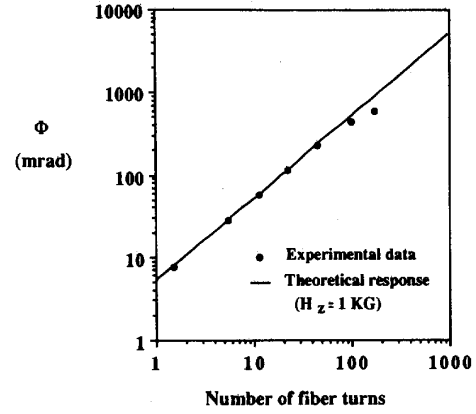


Fig. 6. Measured Faraday rotation angle  $\Phi$  as a function of the number of turns for  $H_z = 1 \text{ KG}$ ,  $H_y = 0$ .

however, that the intrinsic bandwidth of the sensor, limited by the time of flight of the radiation in the coil, is in the range of tens of megahertz [1].

In order to quantify the sensitivity of our sensor to small tolerance errors in  $R$  and  $F$ , we need to compute the parameter  $\mu$  which determines the responsivity reduction, as given by (15) and (16). For example, a decrease in responsivity of no more than 10% (since  $2\mu = 0.9$ ) calls for a corresponding maximum error  $\Delta R$  in the coil radius that can be obtained by the expression  $\mu = \pi N \Delta R / R$ . Thus, for  $N = 100$  a precision of about  $\Delta R = 5 \mu\text{m}$  is required. This figure can surely be obtained in practice, since a typical error for the fiber outer radius, including the coating, is of the order of  $2 \mu\text{m}$ , while even better tolerance is achievable in coiled former manufacturing. Analogously, (17) shows that the required precision in  $F$  amounts to about  $\Delta F = 4 \cdot 10^{-3} \text{ N}$ .

Temperature variations mainly introduce additional tension to the fiber because of the thermal expansion of the former on which the fiber is wound. On the other side, the bending-birefringence variation, due to the radius change  $\Delta R = \alpha R \Delta T$  ( $\alpha$  being the thermal expansion coefficient), is much smaller. The additional force amounts to  $F = (\Delta R / R) E \pi r^2 = \alpha \Delta T E \pi r^2$ , where  $E$  is the Young's modulus of the material.

To minimize the temperature detuning effect, the former should have a thermal coefficient matched to the fiber one. Using a glass cylinder, the Faraday effect was cumulated almost completely for coils of  $N = 100$  turns, as shown in Fig. 6, where the response versus the number of turns for some sensor heads is reported.

If instead a metallic former is used, the additional tension  $F$  can be as high as  $F = 1.63 \text{ N}$  (brass) for a temperature interval  $\Delta T = 100^\circ\text{C}$ , as can be roughly estimated neglecting the buffering action of the coating and the expansion of the fiber itself. This feature was exploited to test experimentally the results of (12). The reduction of the Faraday rotation by a factor  $\sin 2\mu$  was measured using a 44-turn fiber coil on a brass mandrel. The coil radius was intentionally selected larger than the nominal value so that the phase delay per turn was a little less than  $2\pi$  at room temperature. The coil tension was

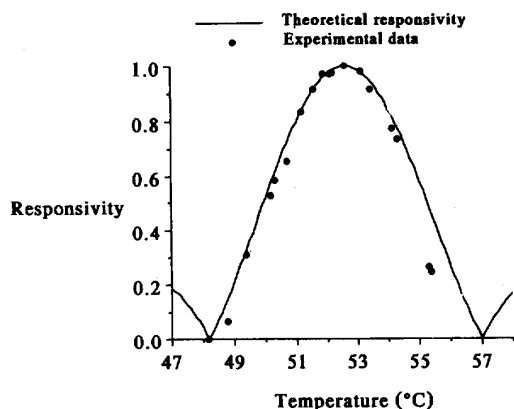


Fig. 7. Experimental test of the sinc  $2\mu$  dependence, obtained by thermo-elastic stress of a 44-turn coil on a brass former. For a glass former, the  $T$  scale is desensitized by a factor of 50 approximately.

varied by heating the former up to 60°C using a Peltier unit with a thermal stabilization. Since the expansion coefficient of the brass is almost two orders of magnitude larger than that of silica, a significant stress was introduced into the fiber even for a moderate change in temperature; in a range of 10°C we could span through the whole central lobe of the sinc function, as shown in Fig. 7.

As a final remark, the use of a high-birefringence fiber, wound with a loop perimeter matching the beat length, would allow to build sensor heads of negligible radial stress. In addition, such sensors would be easier to trim and would have an excellent long term stability. The beat length required for a practical coil (15–25 mm) calls for a special fiber, not currently fabricated but in the easy reach of the present technology.

#### ACKNOWLEDGMENT

The authors wish to thank Prof G. Degli Esposti of the Dipartimento di Ingegneria Elettrica, Università di Pavia, for high voltage testing of their magnetic field meters.

#### REFERENCES

- [1] S. Donati, V. Annovazzi-Lodi, and T. Tambosso, "Magneto-optical fibre sensors for the electrical industry: analysis of performances," *IEE Proc.-J.*, vol. 135, no. 5, pp. 372–382, 1988.
- [2] D. Tang, A. H. Rose, G. W. Day, and S. M. Etzel, "Annealing of linear birefringence in single-mode fiber coils: Application to optical fiber current sensors," *J. Lightwave Technol.*, vol. 9, no. 8, pp. 1031–1037, 1991.
- [3] S. P. Bush and D. A. Jackson, "Dual-channel Faraday-effect current sensor capable of simultaneous measurement of two independent currents," *Opt. Lett.*, vol. 16, pp. 955–957, 1991.
- [4] R. J. Laming and D. N. Payne, "Electric current sensors employing spun highly birefringent optical fibers," *J. Lightwave Technol.*, vol. 7, pp. 2084–2094, 1989.

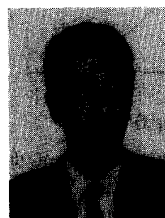
- [5] G. W. Day, D. N. Payne, A. J. Barlow, and J. J. Ramskov-Hansen, "Faraday rotation in coiled, monomode optical fibers: Isolators, filters, and magnetic sensors," *Opt. Lett.*, vol. 7, no. 5, pp. 238–240, 1982.
- [6] V. Annovazzi-Lodi and S. Donati, "Combined reciprocal and nonreciprocal birefringence in optical monomode fibers," *J. Opt. and Quantum Electron.*, vol. 15, pp. 381–388, 1983.
- [7] G. W. Day, D. N. Payne, A. J. Barlow, and J. J. Ramskov-Hansen, "Design and performance of tuned fiber coil isolators," *J. Lightwave Technol.*, vol. LT-2, no. 1, pp. 56–60, 1984.
- [8] M. N. Deeter, A. H. Rose, and G. W. Day, "Fast, sensitive magnetic-field sensors based on the Faraday effect in YIG," *J. Lightwave Technol.*, vol. 8, no. 12, pp. 1838–1842, 1990.
- [9] S. C. Rashleigh, "Origins and control of polarization effects in single-mode fibers," *J. Lightwave Technol.*, vol. LT-1, pp. 312–331, 1983.



**Valerio Annovazzi-Lodi** (M'89) was born in Novara, Italy, on November 7, 1955. He received the degree in Electronic Engineering, cum laude, from the University of Pavia, Pavia, Italy, in 1979.

Since then he has been working at the Department of Electronics of the University of Pavia in the field of electrooptics, formerly on injection modulation phenomena in lasers and on the fiber gyroscope, and later on birefringence effects in optical fibers, fiber sensors, and transmission via diffused infrared radiation. In 1983 he became a staff researcher of the Department of Electronics of the University of Pavia and in 1992 he became an associate professor in the same institution.

Mr. Annovazzi-Lodi is a member of AEI.



**Silvano Donati** (M'75) was born in Milano on August 19, 1942 and graduated in Physics cum laude at the University of Milano in 1966.

From 1966 to 1975 he was with CISE (Milano), carrying out research on noise in photomultipliers and avalanche photodiodes, nuclear electronics, and electrooptic instrumentation. In 1975 he joined University of Pavia, Department of Electronics, where he became full professor of Optoelectronics in 1980. He has worked on laser interferometry, fiber gyroscopes and noise in CCD's and, more recently, on

optical fiber sensors, passive fiber components for telecommunications, and optical interconnections.

Dr. Donati has authored or coauthored about a hundred papers and holds three patents. He is a member of AEI, APS, OSA, ISHM, and has served to organize several national and international meetings and schools in steering and program committees or as a chairman. He also worked in the standardization activity of CEI/IED (CT-76 laser safety).



**Sabina Merlo** was born in Pavia, Italy in 1962. She graduated in Electronic Engineering from the University of Pavia in 1987 and received the M.S.E. in Bioengineering from the University of Washington, Seattle, in 1989. She is presently pursuing the Ph.D. degree in electronic engineering and computer science at the University of Pavia. Since 1988 she has been research assistant, first at the Center for Bioengineering, University of Washington, and then at the Department of Electronics, University of Pavia. Her research work includes fiber-optic sensors for biochemical and electrical applications, and advanced photodetection techniques for fiber-optic telecommunication systems and sensors.

sensors for biochemical and electrical applications, and advanced photodetection techniques for fiber-optic telecommunication systems and sensors.